P H Y S I C A L   R E V I E W   L E T T E R S

Ab Initio Simulation of the Spin Transition during Chemisorption: H/Al(111)

M. Lindenblatt and E. Pehlke*

Institut für Theoretische Physik und Astrophysik, Christian-Albrechts-Universität zu Kiel, 24098 Kiel, Germany

Electronically nonadiabatic effects during the chemisorption of hydrogen atoms on an Al(111) surface are simulated *ab initio* using time-dependent density-functional theory for the electrons in combination with Ehrenfest dynamics for the nuclei. Strongly nonadiabatic effects close to the spin transition of the H atom are identified, and the dissipated energy as well as the electron-hole pair excitation spectra are calculated. The recent Newns-Anderson−model approach by Mizielinski *et al.* is confirmed. The simulations illustrate the physical processes that contribute to internal exoelectron emission.

Energy dissipation constitutes an essential aspect of chemisorption reactions at surfaces. When an atom reacts with a surface, the chemisorption energy, which is released locally, is dissipated. This is believed in many cases to be essentially achieved by phonon excitations. Simulations by Kindt *et al.* [1] have shown that in case of CO/Cu(100) the trapping probability changes only a little when electronic friction effects are accounted for. However, in particular, in the case of very light atoms interacting with a metal surface, part of the chemisorption energy will initially be spent to excite electron-hole pairs in the substrate. In the long run the energy will be further redistributed via various secondary scattering processes, finally resulting in a very slight heating.

Experimentally, electronically nonadiabatic effects during chemisorption are known for long. The emission of exoelectrons into the vacuum due to strongly exothermic reactions has been measured and it has been traced back to charge-transfer processes [2,3]. Moreover chemoluminescence has been observed for a large variety of chemical reactions, ranging from biological systems, like fireflies, to strongly exothermic reactions at alkali metal surfaces [2]. Other systems in which electronically nonadiabatic processes at surfaces have been discussed to be important pertain to the spin-polarization dynamics during the reaction of oxygen molecules with the Al(111) surface [4], electron emission due to the interaction of highly excited NO molecules with metal surfaces [5], the activated adsorption of N_2/Ru(0001) [6], and the sliding friction in case of particular adsorbate/substrate combinations [7]. The interest in chemically excited electrons has recently been intensified by the experiments from McFarland, Nienhaus, and coworkers [8–10]. They deploy Schottky contacts consisting of a thin metal film deposited on a silicon substrate to detect carriers excited by chemisorption reactions. Carriers with sufficient kinetic energy can travel ballistically through the metal film and transverse the Schottky barrier with a certain probability, thereby producing a chemicurrent at no externally applied voltage [11]. The advantage of chemicurrents as opposed to exoelectron emission lies in the fact that the excited electrons do not

have to overcome the large work function barrier of the metal any more, instead they only have to transverse the smaller Schottky barrier of the order of 0.5–1 eV. Thereby it has become feasible to investigate the nonadiabacity of a large number of metal-adsorbate combinations [9]. Likewise the theory of electronic energy dissipation during chemisorption has a long history [12,13]. In case of hydrogen atoms chemisorbing on a metal surface, two effects contribute: nonadiabatic effects due to the electronic spin transfer [14] between the H atom and the substrate, and electronic friction due to the (spin-unpolarized) H atom oscillating in front of the surface [15–18]. In the case of H/Cu(111) the electronic friction coefficient has been calculated by Trail *et al.* [15]; they describe the dissipation within a nearly adiabatic approximation. On the other hand, as detailed by Mizielinski *et al.* [14], the loss of the local electronic spin polarization at the H atom while it approaches the metal surface constitutes a strongly nonadiabatic process that can drive the system far away from the Born-Oppenheimer (BO) surface.

In this Letter, we present, to our knowledge, the first complete *ab initio* molecular dynamic simulations for the electronically nonadiabatic spin-loss transition during chemisorption at metal surfaces. Because of its simple electronic structure, H/Al(111) has been chosen as the model system. Spin-loss transition and electronic friction are described on the same footing, and no suppositions concerning the degree of nonadiabacity have to be made.

We consider the adsorption of an H atom over an Al(111) on-top site. In the simulations, the initially completely spin-polarized H atom is accelerated towards the surface. It gradually loses its spin polarization to the Fermi level of the metal, which acts as a reservoir. After having passed the chemisorption minimum, the H atom is reflected at the top-layer Al atom. Because of energy dissipation, the hydrogen atom becomes trapped, and its dynamics is followed up to the first reflection at the desorption barrier. We note that H chemisorption results in H atoms occupying fcc-hollow sites. The H-atom chemisorption trajectory, which starts above the fcc-hollow site, is rather complicated (the H atom penetrates into the crystal and is re-

flected by an inner Al layer [17,18]) and will not be considered here. The spin transition occurs about 2.6 Å above the top Al layer. At this distance from the surface we expect the corrugation of the electronic coupling strengths not to be very large. Thus the spin-loss transition along the on-top trajectory will be representative also for other adsorption trajectories.

Results from *static* density-functional calculations [19] are summarized in Figs. 1 and 2. Here the Al surface is represented by a slab with a $(\sqrt{3} \times \sqrt{3})$ surface unit cell containing 13 Al layers. Two H atoms have been added to the supercell, one on either side of the slab. H atoms are represented by a $1/r$ Coulomb potential, while a norm-conserving pseudopotential is taken for Al [20]. The generalized gradient approximation by Perdew, Burke, and Ernzerhof [21] is applied to the exchange-correlation energy functional. Sixty-four special **k** points sampling the full Brillouin zone are used. The basis-set cutoff amounts to 20 Ry, which yields a hydrogen chemisorption energy for the Al on-top site of 1.87 eV, compared to a value of 1.90 eV at 40 Ry cutoff.

A cut through the potential-energy surface (PES) for an H atom above the on-top position is shown in Fig. 1. As chemisorbing H atoms move much faster than the Al atoms, all Al coordinates have been frozen in at the positions of the clean surface. At large separations the single electron of the H atom has a local spin moment of 1 (in units of electron spins). Once the H atom approaches the metal surface, its 1s spin orbitals hybridize with the metal Bloch states, shift towards the Fermi level, and broaden. The spin polarization decreases. At the spin-transition point z_S, the ground-state spin polarization vanishes in a second-order–like transition, and the PES of the spin-unpolarized calculation merges with the BO PES [14]. The lifetimes of holes or electrons in the H1s spin orbitals as a function of the distance of the H atom from the surface are shown in Fig. 2. They have been estimated from the Lorentzian width of the peaks in the spin-resolved

H1s-projected density of states, which has been corrected for dispersion effects parallel to the surface caused by the residual interaction between the hydrogen atoms in neighboring unit cells [22]. As the spin transition proceeds via an exchange of electronic spin polarization of the H1s orbital with the bulk, these lifetimes play a crucial role for the dynamics.

To investigate the nonadiabatic dynamics of the spin transition and electronic friction, we have carried through molecular dynamic simulations based on time-dependent density-functional theory (TDDFT) [23]. The time-dependent Kohn-Sham equations are integrated using an extended version of the spin-polarized DFT code [17,19]. The adiabatic approximation is applied to the time-dependent exchange-correlation potential; i.e., the instantaneous spin density is inserted into the static exchange-correlation functional. While this is a common approximation in nonperturbative TDDFT, limitations have to be kept in mind. It is not assumed to provide a satisfying description of electron-electron scattering effects; i.e., we obtain the *initial* electronic excitation spectrum only. Finally, all atoms are assumed to closely follow some classical trajectory—atomic positions obey Ehrenfest dynamics.

The simulations are complicated by the large mass mismatch between electrons and nuclei. The time step of the integration of about 0.002 fs is determined by the rapid motion of the electrons. Therefore convergence parameters have to be relaxed as far as possible without sacrificing the physical model. On the other hand, one parameter, the size of the surface unit cell, even has to be increased with respect to static calculations. The reasoning is that the time-dependent perturbation potential has translational symmetry parallel to the surface. Therefore electronic transitions are vertical in the first Brillouin zone. In the large $2\sqrt{3} \times 2\sqrt{3}$ cell the difference between consecutive Kohn-Sham energy eigenvalues at a fixed k point is sufficiently small in comparison to a typical excitation frequency to obtain a useful description. For this cell we use a 10 Ry basis-set cutoff energy and a single special **k**
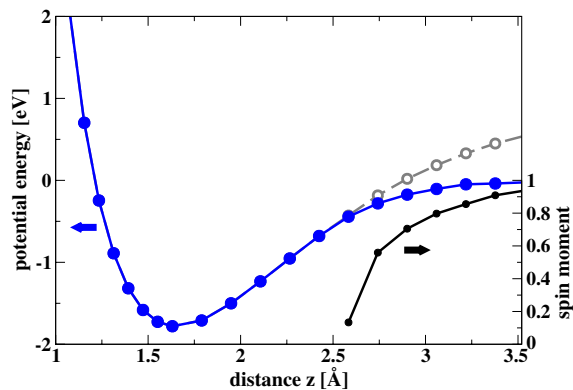

FIG. 1 (color online).   Potential energy and spin moment of a hydrogen atom above the Al(111) on-top position. z is the distance between the H atom and the top-layer Al atom. The spin-relaxed BO surface is denoted by solid circles. The open circles refer to spin-unpolarized calculations.
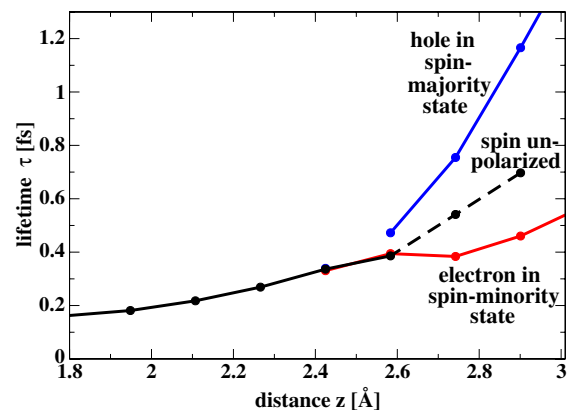

FIG. 2 (color online).   Lifetime of holes or electrons in the H1s orbital as a function of the separation z of the H atom from the top-layer Al atom.
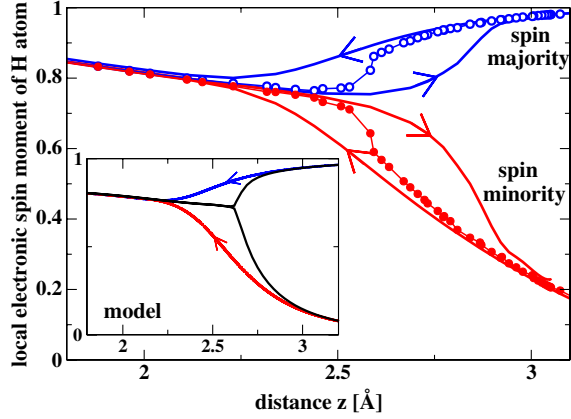
FIG. 3 (color online).   Spin moments $n_\uparrow$, $n_\downarrow$ of the H atom vs its distance z from the surface. Solid lines: nonadiabatic variation from TDDFT molecular dynamics. The arrows denote the direction of the H-atom velocity. Open and solid circles: local spin moments $n_\uparrow$, $n_\downarrow$ in the electronic ground state. The result derived by applying the Newns-Anderson model [14] is shown in the inset.

point. With these convergence parameters the chemisorption energy at the on-top site amounts to 1.78 eV, which still compares reasonably well to the above result for the $\sqrt{3} \times \sqrt{3}$ surface unit cell of 1.9 eV.

The simulations are microcanonical. In particular, the *total* spin moment stays fixed to its initial value. The local polarization at the H atom, however, varies. The electronic density of states close to the Fermi level is sufficiently large to provide a useful reservoir for spin-polarized electrons. Slight finite-size effects are discernible in Fig. 3. The hydrogen atom starts at a position above the Al(111) on-top site, at a distance of 4 Å from the top Al layer, with an initial velocity directed towards the surface which corresponds to an initial kinetic energy of 60 meV. Initially, the electronic system is fully relaxed, the H atom being almost completely spin polarized. When the H atom approaches the surface, the spin polarization is gradually transferred to the Fermi level of the metal substrate. The time-dependent local electronic spin moments at the H atom $n_\uparrow$, $n_\downarrow$ are calculated from the integral over the H1s projected spin density of states up to the Fermi energy. They are compared to the respective local moments in the ground state in Fig. 3. Around the spin-transition point, the dynamics of the system deviates significantly from the BO surface. This occurs also after reflection at the Al atom, when the H atom moves away from the surface. In this case, the H atom reacquires its local spin moment gradually (as opposed to the second-order transition on the BO surface) after it has passed z_S from the inside. Because of the fact that our microcanonical simulation is carried out at fixed total spin moment, the symmetry is broken and the spin polarization at the H atom cannot be flipped after the scattering event. We consider this an artifact of the finite electron reservoir in the supercell calculation; i.e., the simulation cannot yield information about the direction of the local spin
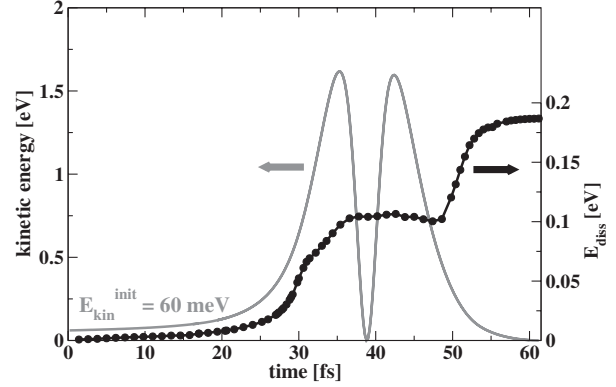

FIG. 4.   Energy E_{diss} dissipated into electron-hole pairs as a function of time t. The kinetic energy of the hydrogen atom is shown for orientation.

polarization after scattering. Both strongly nonadiabatic stages of the spin dynamics are remarkably different due to the topology of $n_\uparrow^{BO}(z)$, $n_\downarrow^{BO}(z)$ shown in Fig. 3. The range of distances z over which the nonadiabatic spin transition occurs is different for H atoms which are approaching or receding from the surface. Finally, we note that for the incoming part of the trajectory, for which a comparison is possible, the TDDFT results are in encouraging agreement with results we have derived by applying Mizielinski's time-dependent Newns-Anderson model [14], using the data from our static DFT calculations.

Nonadiabacity of the spin transition and electronic friction both result in energy dissipation. The energy transferred into electron-hole pair excitations is computed by *a posteriori* relaxing the electronic configurations $|\psi_{j\sigma}(\mathbf{k}, t)\rangle$ down onto the BO surface at fixed atomic coordinates $R(t)$ and fixed total spin moment. The energy gained by this electronic relaxation equals the energy dissipated into electron-hole pairs,
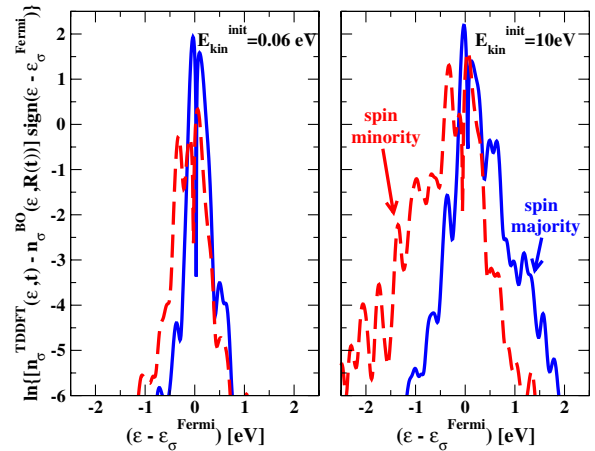

FIG. 5 (color online).   Spin-resolved Kohn-Sham excitation spectra for electrons and holes after the first half-cycle for two different initial kinetic energies of the H atom (solid lines, spin majority; dashed lines, spin minority).

$$E_{\text{diss}}(t) = E_{\text{tot}}^{\text{TDDFT}}(t) - E^{\text{BO}}(R_{\text{ion}}(t)). \qquad (1)$$

For the initial approach of the H atom, E_{diss} amounts to about 0.1 eV, while about another 0.085 eV are dissipated during the way back of the H atom towards the desorption barrier; see Fig. 4. Thus, irrespective of additional phonon losses, already the electronic energy loss enforces sticking. From the strong variation of the energy-dissipation rate we conclude that a considerable portion of the energy dissipation is connected to the spin transition. This is consistent with our previous small value [17] of $E_{\text{diss}} = 0.04$ eV for one oscillation period of an always *spin-unpolarized* H atom in front of the Al surface (with the H atom starting at rest at a distance of 3.2 Å atop the Al atom). Note,

however, that electronic dissipation due to the nonadiabatic spin dynamics will become unimportant as soon as the oscillation amplitude of the H atom has decreased during the course of its motion such that the H atom does not transverse the spin-transition point z_S any more.

While the spin-resolved electron-hole pair excitation spectra after a full cycle of the H atom do not show any discernible spin-dependent features, after the first passage of the H atom through the spin transition, hot spin-majority electrons and hot spin-minority holes can be observed. The spectra displayed in Fig. 5 have been calculated by projecting the $n_{\mathbf{k}\sigma}$ time-dependent states $|\psi_{i\sigma}(\mathbf{k}, t)\rangle$ onto the Kohn-Sham eigenstates $|\phi_{j\sigma}(R(t), \mathbf{k})\rangle$, with eigenenergies $\varepsilon_{j\sigma}(R(t), \mathbf{k})$, after relaxation onto the BO surface at frozen-in atomic coordinates [17],

$$n_\sigma(\varepsilon, t) = \sum_{j\mathbf{k}} w_{\mathbf{k}} \sum_{i=1}^{n_{\mathbf{k}\sigma}} |\langle \psi_{i\sigma}(\mathbf{k}, t)|\phi_{j\sigma}(R(t), \mathbf{k})\rangle|^2 \delta(\varepsilon - \varepsilon_{j\sigma}(R(t), \mathbf{k})). \qquad (2)$$

The integral over the Brillouin zone has been approximated by a sum over special $\mathbf{k}$ points with weights $w_{\mathbf{k}}$, with a single special $\mathbf{k}$ point used in the present simulations. The spectrum consists of a discrete set of eigenenergies and has been convoluted with a Gaussian having a width of 50 meV. The observed abundance of spin-majority electrons with comparatively high energy, as well as high-energy spin-minority holes, is in accordance with the spin-transition mechanism: When the H atom transverses the spin-transition point at z_S, due to the finite electron tunneling probabilities the spin-majority electron resides at the H atom for a while and the system propagates on an excited-state potential-energy surface.

To summarize, we have presented *ab initio* molecular dynamic simulations of nonadiabatic effects occurring during chemisorption of H/Al(111). We find large deviations from adiabacity when the H atom passes through the spin transition, which are well described by the time-dependent Newns-Anderson model of Mizielinski *et al.* The energy dissipated into electron-hole pairs is of the order of 0.1 eV for the first half-cycle of the H atom in front of the surface (one passage of the H atom through the spin transition). The simulations illustrate the physical processes behind the experimentally observed chemicurrents [9,10].

*Electronic address: pehlke@theo-physik.uni-kiel.de
[1] J. T. Kindt, J. C. Tully, M. Head-Gordon, and M. A. Gomez, J. Chem. Phys. **109**, 3629 (1998).
[2] B. Kasemo, Surf. Sci. **363**, 22 (1996).
[3] T. Greber, Surf. Sci. Rep. **28**, 1 (1997).
[4] J. Behler, B. Delley, S. Lorenz, K. Reuter, and M. Scheffler, Phys. Rev. Lett. **94**, 036104 (2005).

[5] J. D. White, J. Chen, D. Matsiev, D. J. Auerbach, and A. M. Wodtke, Nature (London) **433**, 503 (2005).
[6] A. C. Luntz and M. Persson, J. Chem. Phys. **123**, 074704 (2005).
[7] D. Fuhrmann and Ch. Wöll, New J. Phys. **1**, 1 (1998).
[8] H. Nienhaus, H. S. Bergh, B. Gergen, A. Majumdar, W. H. Weinberg, and E. W. McFarland, Phys. Rev. Lett. **82**, 446 (1999).
[9] B. Gergen, H. Nienhaus, W. H. Weinberg, and E. W. McFarland, Science **294**, 2521 (2001).
[10] H. Nienhaus, Surf. Sci. Rep. **45**, 1 (2002).
[11] J. W. Gadzuk, J. Phys. Chem. B **106**, 8265 (2002).
[12] E. Müller-Hartmann, T. V. Ramakrishnan, and G. Toulouse, Phys. Rev. B **3**, 1102 (1971).
[13] K. Schönhammer and O. Gunnarsson, Phys. Rev. B **22**, 1629 (1980); **24**, 7084 (1981).
[14] M. S. Mizielinski, D. M. Bird, M. Persson, and S. Holloway, J. Chem. Phys. **122**, 084710 (2005).
[15] J. R. Trail, M. C. Graham, D. M. Bird, M. Persson, and S. Holloway, Phys. Rev. Lett. **88**, 166802 (2002).
[16] R. Baer and N. Siam, J. Chem. Phys. **121**, 6341 (2004).
[17] J. van Heys, M. Lindenblatt, and E. Pehlke, Phase Transit. **78**, 773 (2005).
[18] M. Lindenblatt, J. van Heys, and E. Pehlke, Surf. Sci. **600**, 3624 (2006).
[19] M. Bockstedte, A. Kley, J. Neugebauer, and M. Scheffler, Comput. Phys. Commun. **107**, 187 (1997); M. Bockstedte (private communication).
[20] M. Fuchs and M. Scheffler, Comput. Phys. Commun. **119**, 67 (1999).
[21] J. P. Perdew, K. Burke, and M. Ernzerhof, Phys. Rev. Lett. **77**, 3865 (1996).
[22] The expectation value for the peak position in the contribution to the H1s projected density of states from every single $\mathbf{k}$ point is calculated and subtracted from the respective Kohn-Sham eigenvalues $\varepsilon_{i\mathbf{k}}$. The width of the resulting peak, which is centered at zero, has been used to estimate lifetimes.
[23] E. Runge and E. K. U. Gross, Phys. Rev. Lett. **52**, 997 (1984).